



## The Fast Prognosis of Inter-Turn Faults in an Induction Motor

Ilham Bouaissi<sup>1\*</sup>, Ali Rezig<sup>1</sup>, Said Touati<sup>2</sup>

<sup>1</sup>L2EI Laboratory, Electrical Engineering Department, Mohamed Seddik Ben Yahia University of Jijel, Jijel 18000, Algeria

<sup>2</sup>Electrical Engineering Department, Nuclear research Centre of Birine, Djelfa 17200, Algeria

Corresponding Author Email: [ilhambouaissi@univ-jjel.dz](mailto:ilhambouaissi@univ-jjel.dz)

<https://doi.org/10.18280/mmep.100418>

### ABSTRACT

**Received:** 12 January 2023

**Revised:** 26 July 2023

**Accepted:** 9 August 2023

**Available online:** 30 August 2023

#### **Keywords:**

*induction motors, forward and backward currents, detection*

This paper introduces a novel approach for detecting and prognosing stator inter-turn faults in induction motors, addressing an important aspect of motor health monitoring. The most commonly employed method for fault detection in this context is Motor Current Signature Analysis (MCSA). By leveraging this method, the paper focuses on the generation of periodic Magneto Motive Force (MMF) waves in the balanced current signal as a result of inter-turn faults. These MMF waves serve as crucial indicators for identifying the presence of such faults. To achieve early detection and prognostic capability for inter-turn faults, the paper proposes a numerical model that relies on analyzing the forward and backward currents. This model offers a promising approach to effectively detect and prognose these faults before they escalate into more severe issues. The obtained results from applying the proposed method demonstrate its efficiency in fault detection and prognostic accuracy for stator inter-turn faults. To validate the effectiveness of the proposed approach, an experimental setup is implemented. This setup provides a real-world context for evaluating the performance and reliability of the method in detecting and prognosing inter-turn faults. Through this validation process, the paper strengthens the credibility and applicability of the proposed technique in practical motor maintenance and fault management scenarios.

## 1. INTRODUCTION

The induction motor (IM) is one of the most used components in industrial applications. Due to this huge concern, several faults can occur during the operation of IM such as broken rotor bars, eccentricity, short-circuited of the stator winding. Etc. Stator inter-turn fault in IMs presents almost 36% of all faults that can occur. It due to the presence of an unbalanced or heavy load and environmental temperature conditions [1-4]. All these circumstances lead to insulation deterioration and huge damage. This type of fault causes a phase imbalance, which has a direct impact on the torque. It starts as short-circuit between turns not detected to arrive at major faults between phases or between phase and ground. As result of a short-circuit between turns, a huge current flowing in the short-circuited part, which leads to an excessive heating of the stator winding. This issue accelerates considerably the degradation of the winding insulation [5].

Many works have been carried out last years on diagnosis; detection and prognosis of short-circuit in IM in recent years.

The wavelet analysis method has been proposed as a new technique to detect the short-circuit inter-ring fault in a rotor coil of an IM. This technique used to extract electrical characteristics under variable conditions of time decomposes the original stator current signals into frequency bands [6-8]. Numerical techniques such as the Finite Elements Method (FEM) are applied to model and simulate electrical machines in both healthy and faulty state and under different load conditions [9-11]. FEM is used to identify stator winding insulation failure and to determine faults' location. Through

signal processing and modeling techniques, it is revealed that the fault can be easily and rapidly detected after its occurrence [12, 13]. In reference [14], the authors have used a high-frequency signal injection that allowed studying the change of fault signature and their values in presence of stator inter-turns. A. Berzoy and al investigated the location stator inter-turn short-circuit on machine parameters. It's shown that the location of inter-turn fault affects the rotating magnetic field shape in the air gap and consequently motor inductances [15]. E. Ghosh and al have proposed a new approach to control the motor and reduce the imbalance caused by inter turn fault [16]. Gyftakis and Cardoso [17] use a spatial vector approach which depends on the higher harmonic index of the park vector. The frequency spectrum of the proposed vector module can be studied and analyzed to extract more information on the gravity of failure. Roy et al. [18] propose a simple technique to detect fault which have been applied to single phase induction motors during operation. The technique is simple and uses few numbers of sensors. Saad et al. [19] propose the use of an extended Kalman filter technique to estimate the percentage of short circuit turns in each phase. This study used in different charges and in the presence of noise. Sundaram and Toliyat [20] use DC voltage injection for monitoring and detection of inter-turn stator faults in five-phase induction motors, integrated into the control loop and allows the motor to smoothly transition from normal operation to fault-tolerant operation once the fault has been detected, with minimal modification of the control logic. The available literature aims, in general, to present the most prominent different techniques for detecting faults in the short circuit [21-25].

In the majority of the methods mentioned earlier, the focus is on detecting inter-turn faults in induction motors during steady-state conditions. However, it is crucial to be able to detect these faults during the motor's starting phase to prevent serious damage. This work proposes a method specifically designed to detect and prognose inter-turn faults in induction motors by monitoring the components of the forward and backward currents that exist in the presence of such defects. The method offers several advantages, particularly in detecting inter-turn faults during the run-up transient operation of the motor. By detecting inter-turn faults early on during motor startup, this method helps prevent damage that could occur if the fault goes unnoticed. Additionally, the amplitude of the forward and backward current components provides valuable information about the severity of the fault, aiding in its prognosis. Another significant advantage of this method is its resilience to variations in motor speed and load. It can effectively differentiate between a short circuit fault and a load variation, which is crucial for accurate fault diagnosis.

In summary, this proposed method addresses the need to detect and prognose inter-turn faults in induction motors during the motor's starting phase. It offers advantages such as fault detection during run-up, severity assessment through current component analysis, and robustness against speed and load variations.

## 2. MATHEMATIC MODEL OF INDUCTION MOTOR WITH INTER-TURN FAULTS

An inter-turn fault in stator winding is introduced as shown in Figure 1. A line is displayed for the stator winding fault.

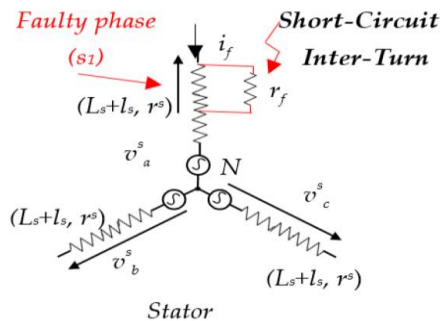


**Figure 1.** Stator windings with inter-turns short-circuit

### 2.1 Voltage equations

From Figure 1 and applying the Kirchhoff Voltage law (KVL) in short-circuited branch, the equation 1 is derived as follow:

$$0 = r_{CC} * i_{CC} + \frac{d\varnothing_{CC}}{dt} \quad (1)$$

where,  $\varnothing_{CC}$  is the flux linkage produced by the short-circuited branch.  $\varnothing_{CC}$  is the resistance which given by:

$$r_{CC} = \mu_{CC} * i_s^{abc} \quad (2)$$

where,  $\mu_{CC}$  the ration of the number of short-circuited turns to the number of the total turns in the phase winding:

$$\mu_{CC} = \frac{N_{CC}}{N_s} \quad (3)$$

By adding Eq. (1) to the system of equations that is derived for the stator winding without fault, a new system of equation is obtained which allow the modeling of IM with inter-turn fault. This system is represented by Eqs. (3) and (4).

$$U_s^{a,b,c} = r_s^{a,b,c} * i_s^{a,b,c} + \frac{d\varnothing_s^{a,b,c}}{dt} \quad (4)$$

### 2.2 The impedance matrix

The stator inductances are given as follow:

$$L_{SS} = \begin{bmatrix} L_d + L_g & -L_d/2 & -L_d/2 \\ -L_d/2 & L_d + L_g & -L_d/2 \\ -L_d/2 & -L_d/2 & L_d + L_g \end{bmatrix} \quad (5)$$

The inductances of the short-circuit part are given by:

$$L_{SCC} = L_d \begin{bmatrix} \cos(\theta_R) \\ \cos(\theta_R + 2\pi/3) \\ \cos(\theta_R - 2\pi/3) \end{bmatrix} \quad (6)$$

where,  $L_d$  and  $L_g$  are the mutual and self-inductance of the stator windings.

### 2.3 Park transformation

Previous research, concerning the use of park's vector approach, has demonstrated the effectiveness of this noninvasive technique for diagnosing malfunctions, such as, single-phasing, open wound-rotor faults, airgap eccentricity and rotor cage faults, in three-phase induction motors.

To minimize the number of model variables, the Concordia transformation is used. It gives  $\alpha \beta$  values from  $a b c$  value by using a three to two axis transformations  $T_{23}$  as:

(1) Concordia transformation of stator current:

$$i_s^{\alpha,\beta} = T_{23} * i_s^{a,b,c} \quad (7)$$

(2) Concordia transformation of rotor current:

$$i_r^{\alpha,\beta} = P(\theta) * T_{23} * i_r^{a,b,c} \quad (8)$$

(3)  $T_{23}$ ,  $P(\theta)$  matrix transformations are defined as:

$$T_{23} = \sqrt{\frac{2}{3}} \begin{bmatrix} \cos(0) & \cos(\frac{2\pi}{3}) & \cos(\frac{4\pi}{3}) \\ \sin(0) & \sin(\frac{2\pi}{3}) & \sin(\frac{4\pi}{3}) \end{bmatrix} \quad (9)$$

$$P(\theta) = \begin{bmatrix} \cos(\theta) & \cos(\theta + \frac{\pi}{2}) \\ \sin(\theta) & \sin(\theta + \frac{\pi}{2}) \end{bmatrix} \quad (10)$$

The short circuit variables are localized on one axis, these projections on the two Concordia axis  $\alpha$  and  $\beta$  is defined as:

$$i_{cc}^{\alpha,\beta} = \begin{bmatrix} \cos(\theta_{cc}) \\ \sin(\theta_{cc}) \end{bmatrix} i_{cc} \quad (11)$$

$$U_s^{\alpha,\beta} = r_s^{\alpha,\beta} * i_s^{\alpha,\beta} + \frac{d\phi_s^{\alpha,\beta}}{dt} \quad (12)$$

$$0 = \mu_{cc} * r_s * i_s^{\alpha,\beta} + \frac{d\phi_{cc}^{\alpha,\beta}}{dt} \quad (13)$$

$$\phi_s^{\alpha,\beta} = (L_m + L_g) * i_s^{\alpha,\beta} + L_m * i_r^{\alpha,\beta} \quad (14)$$

$$\phi_{cc}^{\alpha,\beta} = \sqrt{\frac{2}{3}} * \mu_{cc} * L_m * Q(\theta_{cc}) * (i_s^{\alpha,\beta} + i_r^{\alpha,\beta}) + \left(\frac{2}{3} L_m + L_g\right) \mu_{cc}^2 * Q(\theta_{cc}) * i_{cc}^{\alpha,\beta} \quad (15)$$

where,

$$Q(\theta_{cc}) = \begin{bmatrix} \cos(\theta_{cc})^2 & \cos(\theta_{cc}) \sin(\theta_{cc}) \\ \cos(\theta_{cc}) \sin(\theta_{cc}) & \sin(\theta_{cc})^2 \end{bmatrix} \quad (16)$$

So, after neglecting the leakage inductance  $L_g$  as a function of the magnetizing inductance,  $L_m$  in the short-circuit flux expressions, we can write new flux equations:

$$\phi_s^{\alpha,\beta} = L_m * (i_s^{\alpha,\beta} + i_r^{\alpha,\beta}) = \phi_g^{\alpha,\beta} + \phi_m^{\alpha,\beta} \quad (17)$$

$$\phi_r^{\alpha,\beta} = L_m * (i_s^{\alpha,\beta} + i_r^{\alpha,\beta} + \sqrt{\frac{2}{3}} * i_{cc}^{\alpha,\beta}) = \phi_m^{\alpha,\beta} \quad (18)$$

We define park's transformation as:

$$\begin{bmatrix} i_d \\ i_q \end{bmatrix} = \begin{bmatrix} \cos(\theta) & \sin(\theta) \\ -\sin(\theta) & \cos(\theta) \end{bmatrix} \begin{bmatrix} i_\alpha \\ i_\beta \end{bmatrix} \quad (19)$$

$$\phi_{cc}^{\alpha,\beta} = \sqrt{\frac{2}{3}} * \mu_{cc} * Q(\theta_{cc}) * \phi_m^{\alpha,\beta} \quad (20)$$

### 3. RESULTS AND DISCUSSION

**Table 1.** Three-phase simulated induction motor parameters.

Parameter Name	Symbol	Value	Unit
Stator resistance	$R_1$	2.85	Ohm
Stator resistance	$R_2$	0.482	$\Omega$
Pole pair	$P$	2	-
Resistance of short circuit	$r_f$	22	$\Omega$
Stator inductance	$l_s$	0.73	H
Rotor inductance	$l_r$	0.73	H
Frequency	$f$	50	Hz
Rated power	$P$	1.5	kW
Nominal current(A) in star Y connection	$I$	6.45	A
Nominal voltage(V) in star Y connection	$V$	400	V

The proposed technique is applied in this section. The IM used in the simulation have the parameters shown in Table 1.

Figure 2 and Figure 3 show the simulation results of phases currents in the healthy state, for no load and full load operation condition.

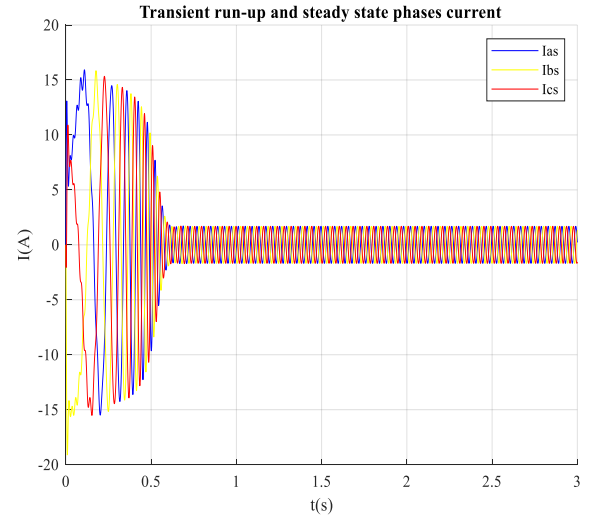


**Figure 2.** Phase current with no-shorted coils and no-load

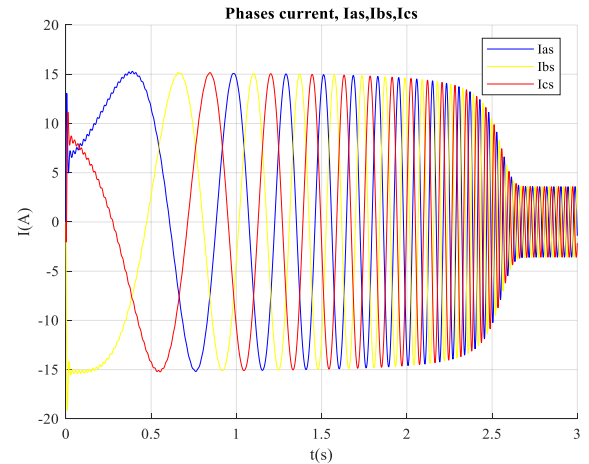


**Figure 3.** Phase current with no-shorted coils and no-load

Figure 3 and Figure 4 show the simulation results of phases currents in the faulty state, for no load and full load condition.

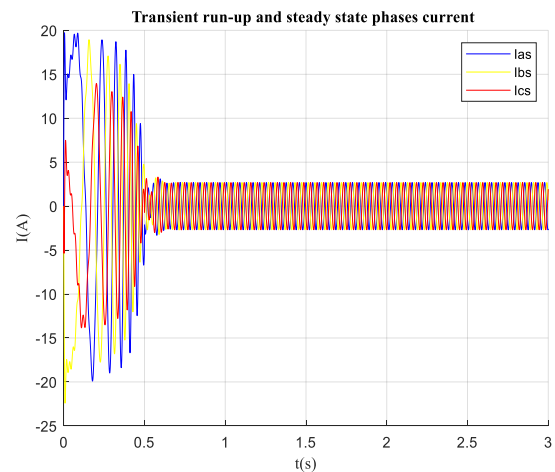


**Figure 4.** Phases current with no-shorted coils full-load

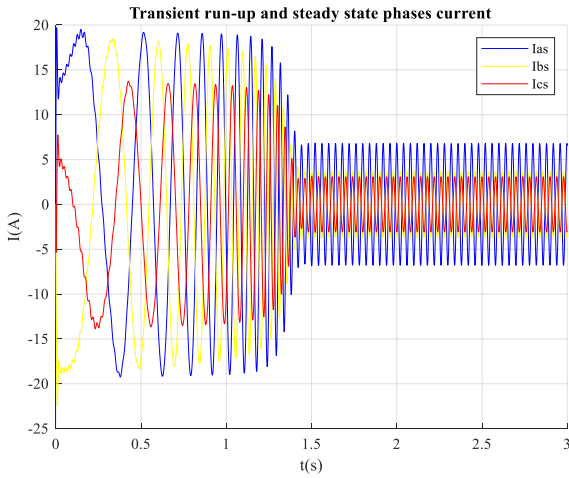


**Figure 5.** Phases current with 20% shorted coils full-load

From Figures 2-5, it is obvious that, the phase current is affected by the inter-turn fault and load change. Unfortunately, it is impossible to distinguish between the presence of an inter-turn fault and load change.

### 3.1 Calculate components forward and backward currents

To differentiate an inter-turn fault from a load change, the proposed technique calculates the forward and the backward component of stator current. Using the above-mentioned park transform, we calculate the forward and backward rotating currents as follows.

$$I_{ff} = \frac{1}{2} \left( (i_{\alpha} + i_{\beta}) \cos(wt) + (i_{\alpha} - i_{\beta}) \sin(wt) \right) \quad (21)$$

$$I_{bb} = \frac{1}{2} \left( (i_{\alpha} - i_{\beta}) \cos(wt) - (i_{\alpha} + i_{\beta}) \sin(wt) \right) \quad (22)$$

Figures 6 and 7 demonstrate the impact of load changes on the phase currents. The magnitude and waveform of the phase currents are influenced by the load, indicating the current requirements to meet the power demand of the system. By analyzing the phase currents, engineers can assess the load conditions and ensure that the system operates within its design limits. It is noteworthy that Figures 6 and 7 show the absence of both forward and backward currents under healthy conditions. In the absence of faults, the forward and backward currents are typically negligible or nonexistent. This indicates that the system is operating as intended, with proper insulation and no abnormal current paths.

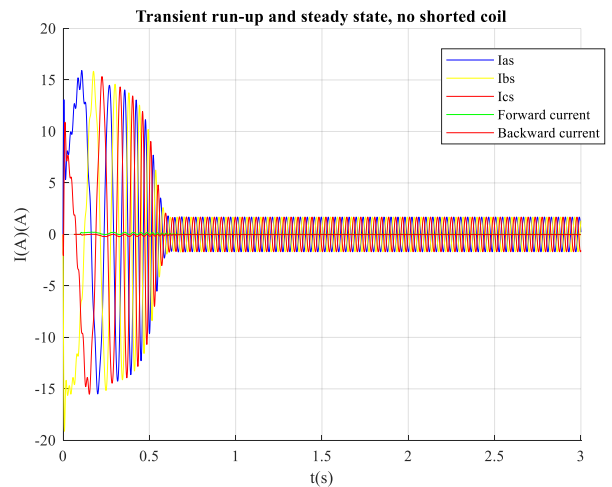
Understanding the behavior of the phase currents under various load conditions provides valuable insights for system analysis, load management, and ensuring reliable operation. The absence of forward and backward currents in healthy cases confirms the absence of faults or abnormal current flow paths, reinforcing the normal and healthy operation of the system.

Figure 8, which presents simulation results for phase currents, forward current, and backward current, provides valuable information regarding the behavior of these currents under different fault conditions. By analyzing this figure, it becomes evident that both the forward and backward currents are observed in the presence of a fault.

During normal operating conditions, the forward current

typically flows in the intended direction, while the backward current remains negligible. However, when a fault occurs, such as a short circuit, the current distribution within the system can be altered. This can result in the appearance of significant forward and backward currents. The forward current, as its name suggests, continues to flow in the expected direction despite the fault. It represents the current that powers the load or operates the system as intended. On the other hand, the backward current arises due to the fault and flows in the opposite direction. It is typically a result of the fault creating a new current path or causing a change in the electrical circuit. The presence of both forward and backward currents in Figure 8 indicates the occurrence of a fault and suggests that a thorough analysis of the fault conditions and their impact on the system is necessary. Further investigation can help identify the fault type, location, and severity, enabling appropriate mitigation measures to be taken.

In the following section, a detailed study of the forward and backward currents observed in Figure 8 will be presented. These currents are of significant interest as they provide valuable insights into the behavior of the system under fault conditions. By analyzing their characteristics and trends, we can gain a better understanding of the fault and its impact on the electrical system.



**Figure 6.** Phases current and forward backward current with no-shorter coils, no-load

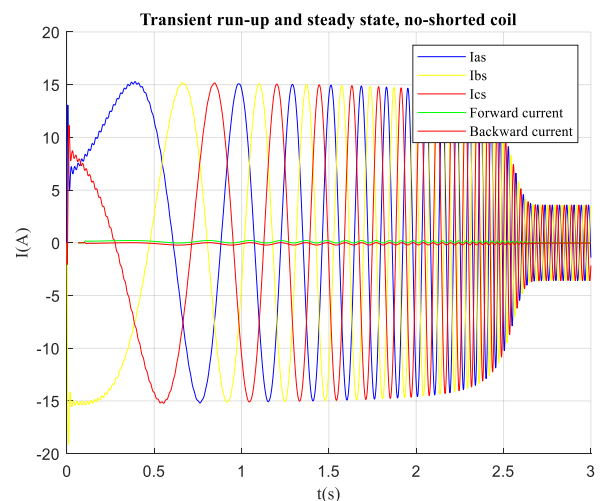


**Figure 7.** Phases current and forward backward current with no-shorter coils, full load

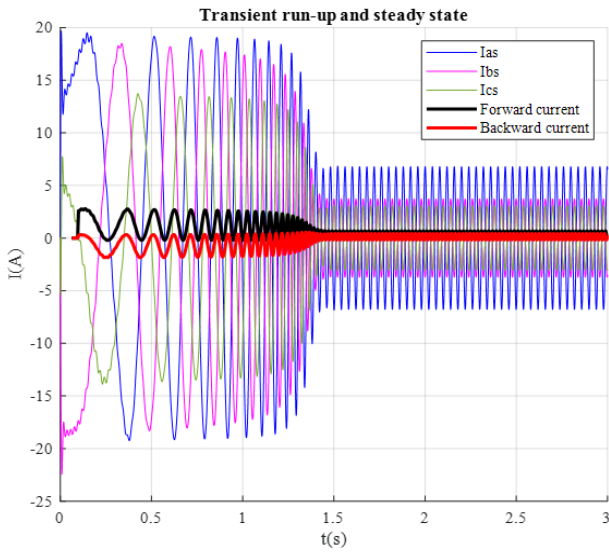


**Figure 8.** Phases current, forward and backward current with no-shorted coils, full-load

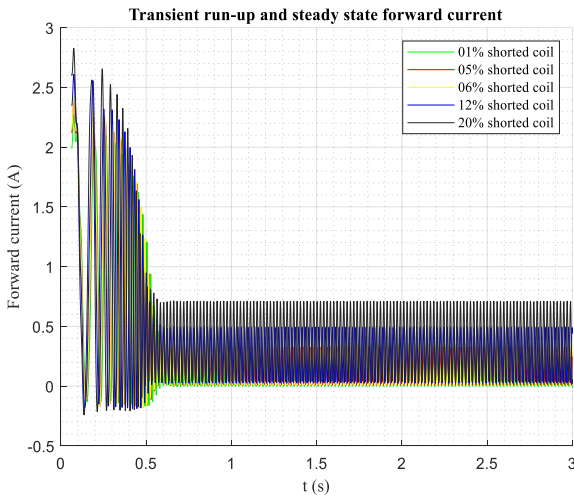


**Figure 9.** Forward current component in transient run-up and steady state with no load for 1%, 05%, 06%, 12% and 20% shorted coils

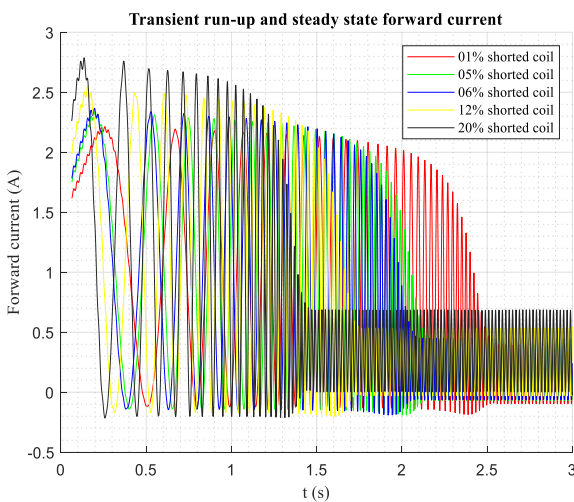


**Figure 10.** Forward current component in transient run-up and steady state with full load for 1%, 05%, 06%, 12% and 20% shorted coils

Figures 9 and 10 show the simulations of forward current in the case of no-load and full-load respectively for different level of defect (1%, 10% and 15% shorted coils). The forward current amplitude increases with defect level.

At this moment 0.3 seconds for no load (Figure 9):

In the case of the coil shorted at 1%, the current is 2.03 (A), in the case of the coil shorted to 06%, the current is 2.16 (A), in the coil is shorted to 12%, the current is 2.30 (A), in the case of the 20% short coil, the current is 2.44 (A).

At the moment 0.3 seconds in relation to the presence of the load (Figure 10):

In the case of a 1% shorted coil, the current intensity is 2.12 (A), in the case of a 06% shorted coil, the current intensity is 2.52 (A), in the case of a 12% shorted coil, the current intensity is 2.68 (A), in the case of a 20% shorted coil, the current intensity is 2.83 (A).

The values of the forward current in the cases of the presence of the load and the absence of the load are very close (with slow time delay in full load condition), indicating that the forward current is not affected by the change of the load. Through this study and the change, we made in the severity of the fault and through the figures shown, it's clear from figures that the forward current appears only when the fault occurs. So the forward current component is one of the most important sign of inter-turn fault.

The increase in forward current amplitude with the severity of the fault serves as a clear indication of the presence and severity of the fault within the system.

By analyzing the forward current behavior under different fault scenarios, you have highlighted its importance in detecting and characterizing inter-turn faults. The correlation between fault severity and forward current amplitude provides valuable insights for fault diagnosis and condition monitoring of the system.

Figures 11 and 12 show the backward current in the case of no-load and full-load respectively for different value of defect (1%, 10%, 15% and 20% shorted coils).

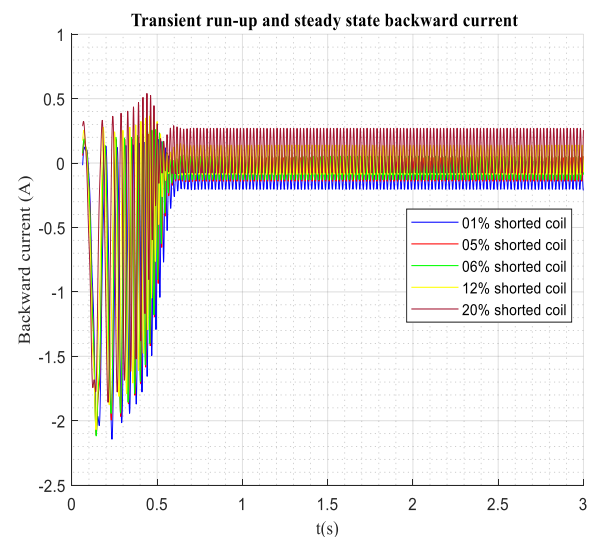


**Figure 11.** Backward current component in transient run-up and steady state with no load for 1%, 05%, 06%, 12% and 20% shorted coils

At the moment 0.2 seconds for no load (Figure 11):

In the case of the coil shorted at 1%, the current is 0.12 (A), in the case of the coil shorted to 06%, the current is 0.22 (A), in the coil is shorted to 12%, the current is 0.25 (A), in the case

of the 20% short coil, the current is 0.35 (A).

The same results are obtained for full load (Figure 12) with slow time delay in full load condition.

The same remarks as for forward current can be made for backward current. However, the backward current variation is not sensitive for small defects.

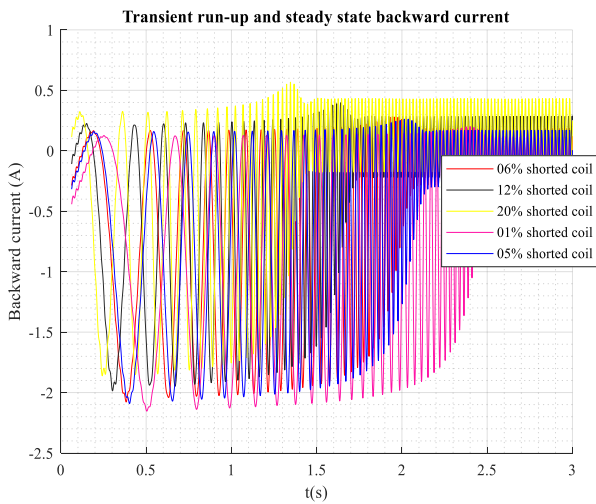


**Figure 12.** Backward current component in transient run-up and steady state at full load for 1%, 05%, 06%, 12% and 20% shorted coils

Through the results obtained, we conclude that the appearance of forward and backward components of currents is a sign of inter-turn defect.

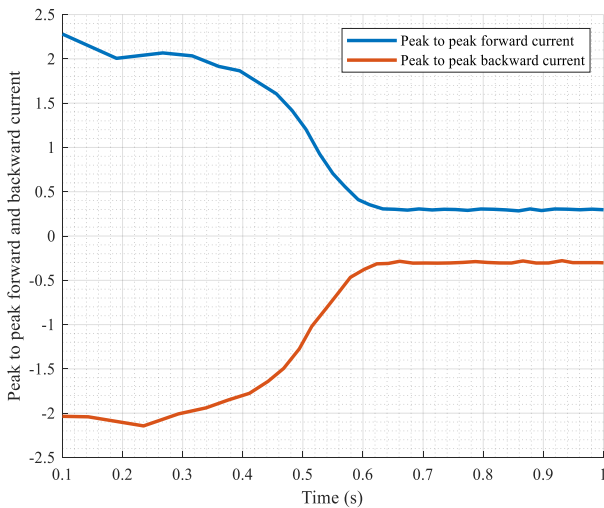


**Figure 13.** Peak to peak forward and backward currents in the 1% shorted coil

Analyzing the deterioration of the forward and backward current values can provide insights into the deterioration of the Insulation Material (IM). Figure 13 presents the trend of value deterioration from peak to peak, highlighting the changes in current over time. By examining these values, it is possible to gain information about the degradation or decline in the performance of the IM.

The forward current refers to the flow of electric current in the intended direction, while the backward current indicates the current flowing in the opposite direction. By monitoring

the peak-to-peak values of these currents, you can assess the changes in the IM's characteristics, such as conductivity or insulation properties.

Deterioration in the forward and backward currents can signify potential issues within the IM. It could indicate insulation breakdown, increased resistance, or other forms of degradation that affect the material's overall performance. By quantifying the deterioration through these current measurements, it becomes possible to track the condition of the IM and take appropriate actions, such as maintenance or replacement, to ensure proper functioning and safety.

#### 4. EXPERIMENTAL INVESTIGATIONS

The experimental bench, which we have exploited to carry out tests on the stator short-circuit fault, is essentially equipped with an asynchronous machine and other equipment and apparatus whose general view is represented in Figure 14.

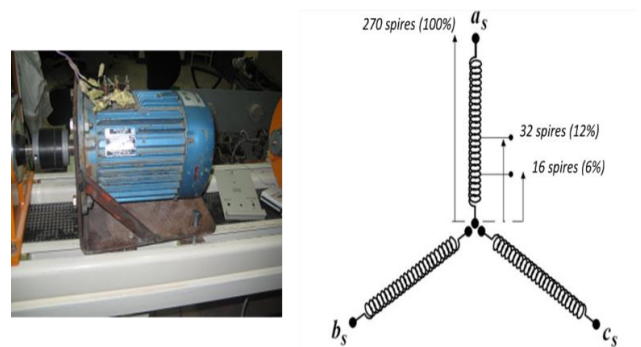


**Figure 14.** Experimental test bench

The machine under test is a 1.5 kw three-phase squirrel cage induction motor. The detailed parameters of the machine are given in previous section (Table 1). The stator of the machine is rewind in a way that can cause a short circuit of 6% and 12%.

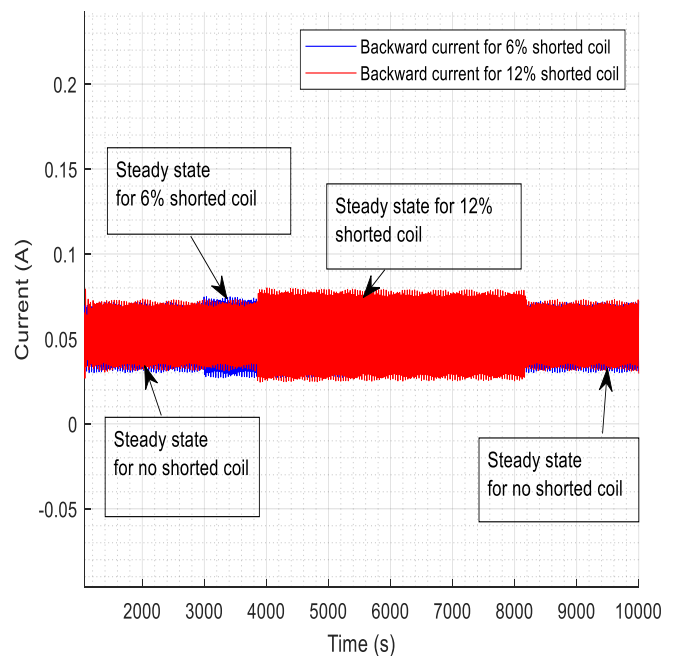


**Figure 15.** Experimental of backward current component in steady state for no-shorted coil, 6% and 12% shorted coils

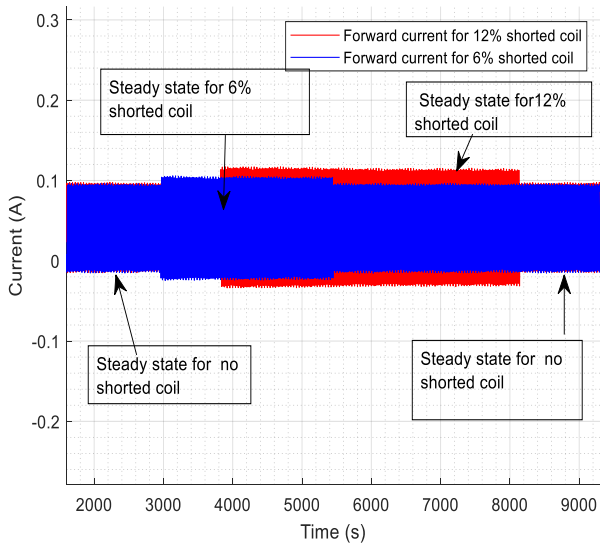


**Figure 16.** Experimental of backward current component in steady state for no-shorted coil, 6% and 12% shorted coils

Figures 15 and 16 show the backward and forward current respectively in steady state for no-shorted coil, 6% and 12% shorted coils. The same remarks as for experimental can be made for simulation. Where we notice an increase in both the forward and backward current with an increase in the shorted coil fault.

## 5. CONCLUSION

This paper discusses the modeling of forward and backward currents to analyze the evolution of faults in the short coil of an induction motor. The findings highlight several important points regarding the behavior of these currents and their relationship to fault detection and prediction. The following observations can be made:

Relationship between fault severity and current amplitude:

The paper demonstrates that as the fault severity increases, both the forward and backward currents exhibit higher amplitudes.

This behavior suggests that the current amplitudes can serve as indicators of fault severity, allowing for the early detection and prediction of defects within the motor.

The increasing current values provide a clear indication of the presence and progression of faults in the short coil.

Absence of forward and backward currents in healthy state:

The absence of forward and backward currents in the healthy state of the motor is an important observation.

This indicates that these currents do not appear under normal operating conditions without any faults, providing a clear distinction between healthy and faulty states.

The absence of currents in the healthy state allows for the early identification of any deviations or abnormalities, making it easier to detect and diagnose faults.

Sensitivity of forward and backward currents to faults:

The paper suggests that the forward current is more sensitive to small faults compared to the backward current.

This implies that even minor faults in the short coil can result in noticeable changes in the forward current, making it a valuable indicator for early fault detection.

The sensitivity difference between the forward and backward currents provides insights into the fault evolution

and can aid in developing accurate fault diagnosis techniques.

Consistency between modeling and experimental results:

The comment also mentions that the results of the experiments align with the observations made in the modeling phase.

This consistency between the modeling and experimental findings strengthens the validity of the conclusions and reinforces the understanding of the forward and backward current behaviors in the presence of faults.

By considering the modeling and experimental results, the paper contributes to the understanding of fault evolution in the short coil of an induction motor. The emphasis on the forward and backward currents as indicators of faults, their relationship with fault severity, and the absence of currents in the healthy state highlight their importance for early fault detection and prediction.

## REFERENCES

- [1] Gheitasi, A., Al-Anbuky, A., Lie, T.T. (2011). Impact of propagation of fault signals on industrial diagnosis using current signature analysis. AUPEC 2011, Brisbane, QLD, Australia, pp. 1-6.
- [2] Xu, Z., Hu, C.H., Yang, F., Kuo, S.H., Goh, C.K., Gupta A., Nadarajan S. (2017). Data-driven inter-turn short circuit fault detection in induction machines. IEEE Access, 5: 25055-25068. <https://doi.org/10.1109/ACCESS.2017.2764474>
- [3] Zorig, A., Kia, S.H., Chouder, A., Rabhi, A. (2022). A comparative study for stator winding inter-turn short-circuit fault detection based on harmonic analysis of induction machine signatures. Mathematics and Computers in Simulation, 196: 273-288. <https://doi.org/10.1016/j.matcom.2022.01.019>
- [4] Raj, K.K., Joshi, S.H., Kumar, R. (2021). A state-space model for induction machine stator inter-turn fault and its evaluation at low severities by PCA, In 2021 IEEE Asia-Pacific Conference on Computer Science and Data Engineering (CSDE), Brisbane, Australia, pp. 1-6. <https://doi.org/10.1109/CSDE53843.2021.9718479>
- [5] Eldeeb, H.H., Zhao, H., Mohammed, O. (2020). Effect of stator's insulation failure on the performance of motor drive system. In 2020 International Applied Computational Electromagnetics Society Symposium (ACES), Monterey, CA, USA, pp. 1-2. <https://doi.org/10.23919/ACES49320.2020.9196081>
- [6] Athulya, K. (2018). Inter turn fault diagnosis in wound rotor induction machine using wavelet transform. In 2018 International CET Conference on Control, Communication, and Computing (IC4), Thiruvananthapuram, India, pp. 22-27. <https://doi.org/10.1109/CETIC4.2018.8530887>
- [7] Keravand, M., Faiz, J., Soleimani, M., Ghasemi-Bijan, M., Bandar-Abadi, M., Cruz, S.M. (2017). A fast, precise and low-cost stator inter-turn fault diagnosis technique for wound rotor induction motors based on wavelet transform of rotor current. In 2017 IEEE 11th International Symposium on Diagnostics for Electrical Machines, Power Electronics and Drives (SDEMPED), Tinos, Greece, pp. 254-259. <https://doi.org/10.1109/DEMPEP.2017.8062364>
- [8] Siddiqui, K.M., Sahay, K., Giri, V.K. (2016). Early diagnosis of stator inter-turn fault in inverter driven

- induction motor by wavelet transform. In 2016 IEEE 1st International Conference on Power Electronics, Intelligent Control and Energy Systems (ICPEICES), Delhi, India, pp. 1-6. <https://doi.org/10.1109/ICPEICES.2016.7853647>
- [9] Chen, Y., Wang, L., Wang, Z., Rehman, A.U., Cheng, Y., Zhao, Y., Tanaka, T. (2015). FEM simulation and analysis on stator winding inter-turn fault in DFIG. In 2015 IEEE 11th International Conference on the Properties and Applications of Dielectric Materials (ICPADM), Sydney, NSW, Australia, pp. 244-247. <https://doi.org/10.1109/ICPADM.2015.7295254>
- [10] Mellah, H., Arslan, S., Sahraoui, H., Hemsas, K.E. (2022). The effect of stator inter-turn short-circuit fault on DFIG performance using FEM. *Engineering, Technology & Applied Science Research*. <https://ssrn.com/abstract=4111342>.
- [11] Abdesselam, L., Ammar, M., Guy, C. (2011). Analysis of inter-turn short circuit in slots by finite element model. In IEEE 10th International Conference on Environment and Electrical Engineering, Rome, Italy, pp. 1-4. <https://doi.org/10.1109/EEEIC.2011.5874589>
- [12] Malekpour, M., Phung, B.T., Ambikairajah, E. (2018). Modelling and diagnostic of incipient stator inter-turn short circuit fault in induction motors. In IEEE Condition Monitoring and Diagnosis (CMD), Perth, WA, Australia, pp. 1-6. <https://doi.org/10.1109/CMD.2018.8535624>
- [13] Gyftakis, K.N., Marques-Cardoso, A.J. (2019). Reliable detection of very low severity level stator inter-turn faults in induction motors. In IECON 45th Annual Conference of the IEEE Industrial Electronics Society, Lisbon, Portugal, 1: 1290-1295. <https://doi.org/10.1109/IECON.2019.8926928>
- [14] Otero, M., Bossio, G.R., de la Barrera, P.M., Tyshakin, O., Leidhold, R. (2018). Inter-turn faults detection in Induction Motor drives using zero-sequence signal injection. In 2018 International Symposium on Power Electronics, Electrical Drives, Automation and Motion (SPEEDAM), Amalfi, Italy, pp. 202-207. <https://doi.org/10.1109/SPEEDAM.2018.8445411>
- [15] Berzoy, A., Mohamed, A.A.S., Mohammed, O. (2017). Impact of inter-turn short-circuit location on induction machines parameters through FE computations. *IEEE Transactions on Magnetics*, 53(6): 1-4. <https://doi.org/10.1109/TMAG.2017.2665639>
- [16] Ghosh, E., Mollaiean, A., Kim, S., Tjong, J., Kar, N.C. (2017). Intelligent flux predictive control through online stator inter-turn fault detection for fault-tolerant control of induction motor. IEEE International Conference on Industrial Technology (ICIT), Toronto, ON, Canada, pp. 306-311. <https://doi.org/10.1109/ICIT.2017.7913101>
- [17] Gyftakis, K.N., Cardoso, A.M. (2017). A new space vector approach to detect stator faults in induction motors. IEEE Workshop on Electrical Machines Design, Control and Diagnosis (WEMDCD), Nottingham, UK, pp. 232-237. <https://doi.org/10.1109/WEMDCD.2017.7947752>
- [18] Roy, R.K., Chatterjee, A., Chatterjee, D. (2016). A current signature-based stator main winding fault detection technique for single-phase induction machine. IEEE, 2nd International Conference on Control, Instrumentation, Energy & Communication (CIEC), Kolkata, India, pp. 284-288. <https://doi.org/10.1109/CIEC.2016.7513837>
- [19] Saad, W.W., Abd El-Geliel, M., Lotfy, A. (2017). IM stator winding faults diagnosis using EKF. IEEE, Conf on Advanced Control Circuits Systems (ACCS) Systems & 2017 Intl Conf on New Paradigms in Electronics & Information Technology (PEIT), Alexandria, Egypt, pp. 34-39. <https://doi.org/10.1109/ACCS-PEIT.2017.8302997>
- [20] Sundaram, V.M., Toliyat, H.A. (2016). Stator inter-turn fault detection for seamless fault-tolerant operation of five-phase induction motors. IEEE Energy Conversion Congress and Exposition (ECCE), pp. 1-8. <https://doi.org/10.1109/ECCE.2016.7855466>
- [21] Bento, F., Adouni, A., Muxiri, A.C., Fonseca, D.S., Marques Cardoso, A.J. (2021). On the risk of failure to prevent induction motors permanent damage, due to the short available time - to - diagnosis of inter - turn short - circuit faults. *IET Electric Power Applications*, 15(1): 51-62. <https://doi.org/10.1049/elp2.12008>
- [22] Mesai-Ahmed, H., Jlassi, I., Cardoso, A.J.M., Bentaallah, A. (2021). Multiple open-circuit faults diagnosis in six-phase induction motor drives using stator current analysis. *IEEE Transactions on Power Electronics*, 37(6): 7275-7285. <https://doi.org/10.1109/TPEL.2021.3132236>
- [23] Otero, M., de la Barrera, P.M., Bossio, G.R., Leidhold, R. (2020). Stator inter - turn faults diagnosis in induction motors using zero - sequence signal injection. *IET Electric Power Applications*, 14(14): 2731-2738. <https://doi.org/10.1049/iet-epa.2020.0461>
- [24] Raj, K.K., Joshi, S.H., Kumar, R. (2021). A state-space model for induction machine stator inter-turn fault and its evaluation at low severities by PCA. In IEEE Asia-Pacific Conference on Computer Science and Data Engineering (CSDE), Brisbane, Australia, pp. 1-6. <https://doi.org/10.1109/CSDE53843.2021.9718479>
- [25] Berzoy, A., Eldeeb, H.H., Mohammed, O. (2018). Online fault detection of stator winding faults in IM driven by DTC using the off-diagonal term of the symmetrical component impedance matrix. In 2018 IEEE Applied Power Electronics Conference and Exposition (APEC), San Antonio, TX, USA, pp. 2482-2487. <https://doi.org/10.1109/APEC.2018.8341366>